DYNAMIC INSTABILITY OF FLUID FILLED CIRCULAR CYLINDRICAL SHELLS

P. B. Gonçalves
Pontifical University of Rio de Janeiro – PUC - Rio, Civil Enegineering Department. 22453-900 - Rio de Janeiro - Brazil
paulo@civ.puc-rio.br

Z. J. G. N. del Prado
F. M. A. Silva
Federal University of Goiás, UFG, Civil Engineering Department. 74605-220 – Goiânia, GO, Brazil
zenon@eec.ufg.br

Abstract. *This paper discusses the dynamic instability of fluid filled cylindrical shells subjected to time dependent axial edge loads. In the present paper a simplified low dimensional model, which retains the essential non-linear terms, is used to study the non-linear oscillations and instabilities of the shell. For this, Donnell's shallow shell equations are used together with the Galerkin method to derive a set of coupled non-linear ordinary differential equations of motion, which are in turn, solved by the Runge-Kutta method. To study the non-linear behavior of the shell, several numerical strategies were used to obtain Poincaré map and bifurcation diagrams. Special attention is given to the influence of the fluid on the escape boundaries. The numerical results obtained in this investigation clarify the conditions where instability may occur and help to derive safe design criteria for these shells under dynamic loads.*

Keywords. *Dynamic instability, cylindrical shells, non-linear vibrations, fluid-structure interaction*

1. Introduction

Thin-walled cylindrical shells are widely used in many industries. Due to increasing use of high-strength materials, the use of sophisticated numerical techniques and optimization methods in analysis, the design of such shells is often buckling-critical. In many circumstances these shells are subjected not only to static loads but also to dynamic disturbances and filled with internal fluid. However, thin-walled cylindrical shells when subjected to axial compressive loads often exhibit a highly nonlinear behavior with a high imperfection sensitivity and may loose stability at loads levels as low as a fraction of the material's strength.

Many studies are concentrated on the analysis of shells vibrating in vacuum and much less is focused on the analysis of the nonlinear vibrations of cylindrical shells in contact with a dense fluid. One of the first studies on vibrations of circular cylindrical shells in contact with a dense fluid considering shell nonlinearity was published by Ramachandran (1979). He studied the large-amplitude vibrations of circular cylindrical shells having circumferentially varying thickness and immersed in a quiescent, inviscid and incompressible fluid using the Donnell's shell theory.

Boyarshina (1984, 1988) studied theoretically the nonlinear free and forced vibrations and stability of a circular cylindrical tank partially filled with a liquid and having a free surface. Here, nonlinearity is attributed to the interaction of free surface waves and elastic flexural vibrations of the shell.

Gonçalves and Batista (1988) considered simply supported circular cylindrical shells filled with incompressible fluid. For modeling the shell, Sanders nonlinear theory and a novel modal expansion that includes two terms in the radial direction (the asymmetric and the axisymmetric ones) and ten terms to describe the in-plane displacements were used. Numerical results were obtained concerning the effect of the liquid on the nonlinear behavior of shells. It was found that the presence of a dense fluid leads to more strong softening results vis-a-vis those for the same shell in vacuum.

Chiba (1993b) studied experimentally the large-amplitude vibrations of two vertical cantilevered circular cylindrical shells made of a polyester sheet partially filled with different levels of water. He observed that for bulging modes with the same axial wave number, the weakest degree of softening nonlinearity can be attributed to the mode having the minimum natural frequency, as observed for the same empty shells. He also found that shorter tanks have a larger softening nonlinearity than taller ones, as in vacuum. The tank with a lower liquid height has a greater softening nonlinearity than the tank with a higher liquid level.

Amabili et al (1998) studied the nonlinear free and forced vibrations of a simply supported, circular cylindrical shell in contact with an incompressible and inviscid, quiescent dense fluid. Donnell's nonlinear shallow-shell theory is used. The boundary conditions on radial displacement and continuity of circumferential displacement are exactly satisfied, while axial constraint is satisfied "on the average". The problem is reduced to a system of ordinary differential equations by means of the Galerkin method, assuming an appropriate deflection shape. The mode shape is expanded by using two asymmetric modes (driven and companion modes) plus the axisymmetric mode.

In the present study, a low dimensional model, which retains the essential nonlinear terms is used to study then nonlinear oscillations and instabilities of the shell. Here the interest is focused on a pivotal interaction between non-symmetric and axi-symmetric modes, which produce escape from the pre-buckling potential well. To discretize the shell, Donnell shallow shell equations, modified with the transverse inertia force, are used together with Galerkin method to derive a set of coupled ordinary differential equations of motion, which are, in turn, solved by the Runge-

Kutta method. In order to study the nonlinear behavior of the shell, several numerical strategies were used to obtain time responses, Poincaré maps and bifurcation diagrams.

The fluid is modeled as non-viscous and incompressible and its motion is assumed to be irrotational. As a result, it can be characterized by a velocity potential. The solution for the velocity potential is taken as a sum of suitable functions, the unknown parameters of which are determined by the kinetic condition along the wetted surface of the shell (Batista and Gonçalves, 1988).

2. Problem Formulation

2.1 Shell Equations

Consider a perfect thin-walled fluid filled circular cylindrical shell of radius R, length L, and thickness h. The shell is assumed to be made of an elastic, homogeneous, and isotropic material with Young’s modulus E, Poisson ratio ν, and mass per unit area M. The axial, circumferential and radial co-ordinates are denoted by, respectively, *x*, *y* and *z*, and the corresponding displacements on the shell surface are in turn denoted by U, V, and W, as shown in Figure 1.

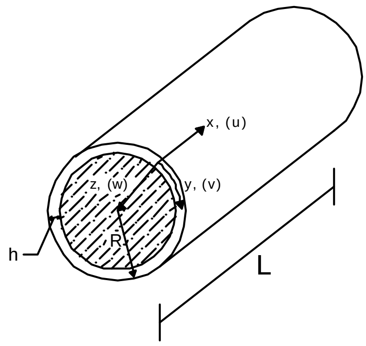

Figure 1. Shell geometry and coordinate system.

The shell is subjected to a uniformly distributed axial load of the form:

$$P(t) = P_o + P_1 \cos(\boldsymbol{w}t) \tag{1}$$

where P_o is the uniform static load applied along the edges x=0, L, P_1 is the magnitude of the harmonic load, t is time and ω is the forcing frequency.

The nonlinear equations of motion based on the Von Karmán-Donnell shallow shell theory, in terms of a stress function *f* and the transversal displacement *w* are given by:

$$M\,\ddot{w} + b_1\dot{w} + b_2\nabla^4\dot{w} + D\nabla^4 w = p_h R + F_{,yy}\,w_{,xx} + F_{,xx}\left(w_{,yy} + \frac{1}{R}\right) - 2F_{,xy}\,w_{,xy} \tag{2}$$

$$\frac{1}{Eh}\nabla^4 f = -\frac{1}{R}w_{,xx} - w_{,xx}w_{,yy} + w_{,xy}^2 \tag{3}$$

where:

$$F = f^F + f \qquad\qquad f^F = -\frac{1}{2}P_0 y^2 \tag{4}$$

and p_h is the fluid pressure, ∇^4 is the biharmonic operator, b_1 and b_2 are damping coefficients and *D* is the flexural rigidity defined as:

$$D = E\,h^3 / 12\left(1 - n^2\right) \tag{5}$$

In the foregoing, the following non-dimensional parameters have been introduced:

$$W = \frac{w}{h} \qquad V = \frac{x}{L} \qquad q = \frac{y}{R} \qquad t = w_o t \qquad \Omega = \frac{w}{w_0}$$

$$\bar{f} = \frac{R}{E h^2 L^2} f \quad \Gamma_o = \frac{P_0}{P_{cr}} = \frac{R\sqrt{3\left(1-n^2\right)}}{E h^2} P_o \qquad \Gamma_1 = \frac{P_1}{P_{cr}} = \frac{R\sqrt{3\left(1-n^2\right)}}{E h^2} P_1 \tag{6}$$

and ω_o is the lowest natural frequency of the empty shell.

2.2 Modal Analysis

The numerical model is developed by expanding the transversal displacement component *w* in series in the circumferential and axial variables. From previous investigations on modal solutions for the non-linear analysis of cylindrical shells under axial loads (Hunt et al. 1986; Gonçalves and Batista, 1988; Gonçalves and Del Prado, 2002) it is observed that, in order to obtain a consistent modeling with a limited number of modes, the sum of shape functions for the displacements must express the non-linear coupling between the modes and describe consistently the unstable post-buckling response of the shell as well the correct frequency-amplitude relation.

The lateral deflection *w* can be generally described as (Gonçalves and Batista, 1988):

$$W = \sum_{i=1,3,5} \sum_{j=1,3,5} W_{ij} \cos\left(i n q\right) sin\left(j m p\ V\right) + \sum_{k=0,2,4} \sum_{l=0,2,4} W_{ij} \cos\left(k\, n q\right) sin\left(l\, m p\ V\right) \tag{7}$$

where n is the number of waves in the circumferential direction of the basic buckling or vibration mode, m is the number of half-waves in the axial direction, $q = y/R$ and $V = x/L$.

These modes represent both the symmetric and asymmetric components of the shell deflection pattern. The first double series represents the unsymmetrical modes with odd multiples of the basic wave numbers *m* and *n*. The second double series represents, besides the asymmetric modes which contains an even multiple of the basic wave numbers *m* and *n* and rosette modes, the axy-simmetric modes which play an important role in the non-linear modal coupling and loss of stability of the shell.

Previous studies on buckling of cylindrical shells have shown that the most important modes are the basic buckling or vibration mode and the axi-symmetric mode with twice the number of half waves in the axial direction as the basic mode, that is:

$$W = x\left(t\right)_{11} \cos\left(n q\right) \mathrm{sen}\left(m p\ V\right) + x\left(t\right)_{02} \cos\left(2 m p\ V\right) \tag{8}$$

The relevance of these modes from a physical point of view is explained by Croll and Batista (1981) and from symmetry and catastrophe theory arguments by Hunt et al. (1986). These modes are enough to describe the initial post-buckling behavior of the shell as well as the topology of the pre-buckling well and the potential barrier connected with the unstable equilibrium positions lying on the initial post-buckling path.

Substituting the assumed form of the lateral deflection Eq. (8) on the right-hand side of the compatibility Eq. (3) one may solve the resulting equation for the stress function *f* in terms of *w* together with the relevant boundary and continuity conditions. Upon substituting the modal expressions for *f* and *w* into Eq. (2) and applying the Galerkin method, a set of non-linear ordinary differential equations is obtained in terms of modal amplitudes $\xi(\tau)_{ij}$.

2.3 Fluid Equations

The shell is assumed to be completely fluid-filled. The irrotational motion of an incompressible and non-viscous fluid can be described by a velocity potential $f\left(x, r, q, t\right)$. This potential function must satisfy the Laplace equation, which can be written in dimensionless form as:

$$\bar{f}_{,xx} + \frac{1}{k}\bar{f}_{,k} + \frac{1}{k^2}\bar{f}_{,qq} + \bar{f}_{,kk} = 0 \tag{9}$$

where $k = r/R$ and $\bar{f} = g\, f/R^2$.

The influence of the nonlinearities is, in terms of the fluid, very small, then we can adopt the fluid as linear. Therefore the hydrodynamic fluid pressure will be given by:

$$p_h = x_{11,tt}\, m_a \cos\left(n q\right) sin\left(m p\ x\right) \tag{10}$$

where m_a is the additional mass depending on the fluid contained in shell, which is given by:

$$m_a = (\rho_f\ R)\left\{m\pi\xi\left[\frac{I_{n-1}(m\pi V)}{I_n(m\pi V)} - \frac{n}{m\pi V}\right]\right\}^{-1} \tag{11}$$

where ρ_F is the density of the fluid, ρ_S is the shell material density and I_{n-1} and I_n are Bessel functions.

3. Results

Consider a thin-walled cylindrical shell with h=0,002 m, R=0,2 m, L=0,4 m, E=2,1x10^8 kN/m2, ν=0,3, M=78,5 kg/m^2, $\beta_1=2\varepsilon M\omega_o$ with ε=0,003 and $\beta_2=\eta D$ with η=0,0001. The densities ρ_s=7850 kg/m^3 and ρ_f=1000 kg/m^3. For this shell geometry the lowest natural frequency occurs for *(n,m)=(5,1).*

Now the parametric instability and escape of the fluid-filled cylinder under axial harmonic forcing, as described by Eq. (2), will be considered. In the following, the constant part to the loading Γ_o is assumed to lie between the upper and lower critical load in the static case.

Figure 2 shows the numerically obtained bifurcation boundaries for a slowly evolving system in (frequency of excitation, amplitude of excitation) control space for Γ_o=0,80 and Γ_o=0,40. The lower stability boundary corresponds to parameter values for which small perturbations from the trivial solution will result in an initial growth in the oscillation; therefore it defines the parametric instability boundary. The second limit corresponds to escape from the pre-buckling potential well in a slowly evolving system. These curves were obtained by increasing slowly the amplitude while holding the frequency constant. As one can observe, the parametric stability boundary is composed of various “curves”, each one associated with a particular bifurcation event. The deepest well is associated with the principal instability region at $\omega=2\omega_p$, while the second well to the left is the secondary instability region occurring around $\omega=\omega_p$ and the other smaller wells to the left are connected with super-harmonic resonances. The horizontal dotted line corresponds to the static critical load for this shell. Comparing figures (a) and (b), one can conclude that the static pre-loading has the effect of lowering the stability boundaries, of enlarging the width parameters of the instability regions and of shifting the instability regions to the left. In both cases the instability boundaries can be much lower than the static critical load.

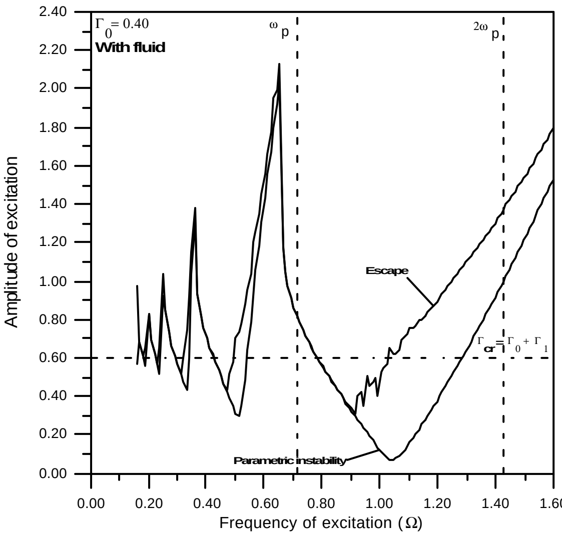

(a) Γ_o=0,40

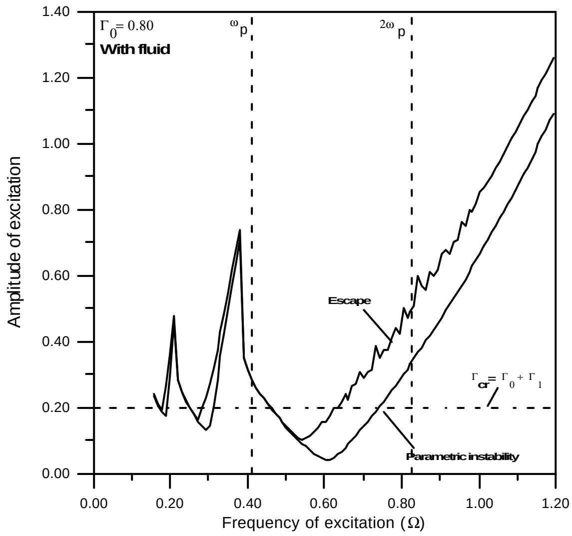

(b) Γ_o=0,80

Figure 2. Instability boundaries in control space.

Figures 3 and 4 show typical bifurcation diagrams connected with the principal instability region due to the variation of parameter Γ_1, for different values of Ω. The bifurcation diagrams where obtained by brute force method and in these figures the amplitude ξ_{11} is plotted as a function of the forcing amplitude, Γ_1.

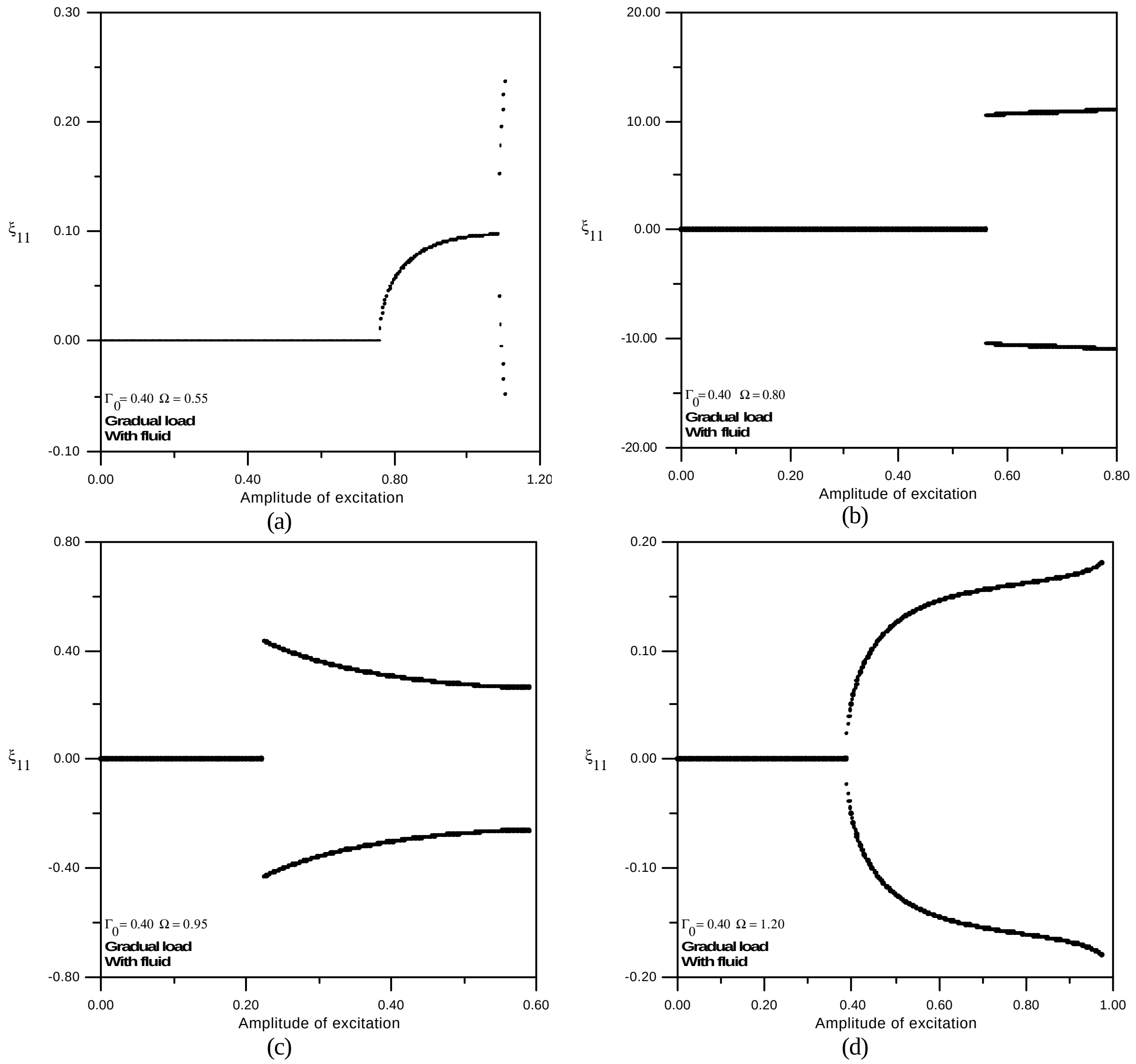

Figure 3. Bifurcation diagrams of the Poincaré map for water filled shell. Principal instability region, Γ_o=0,40.

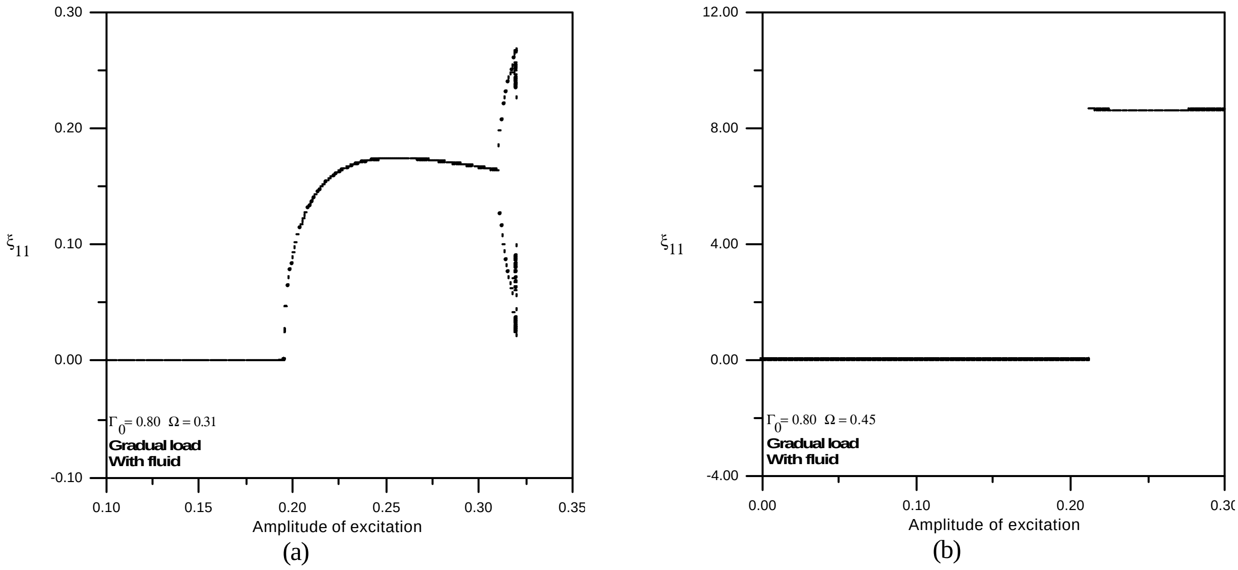

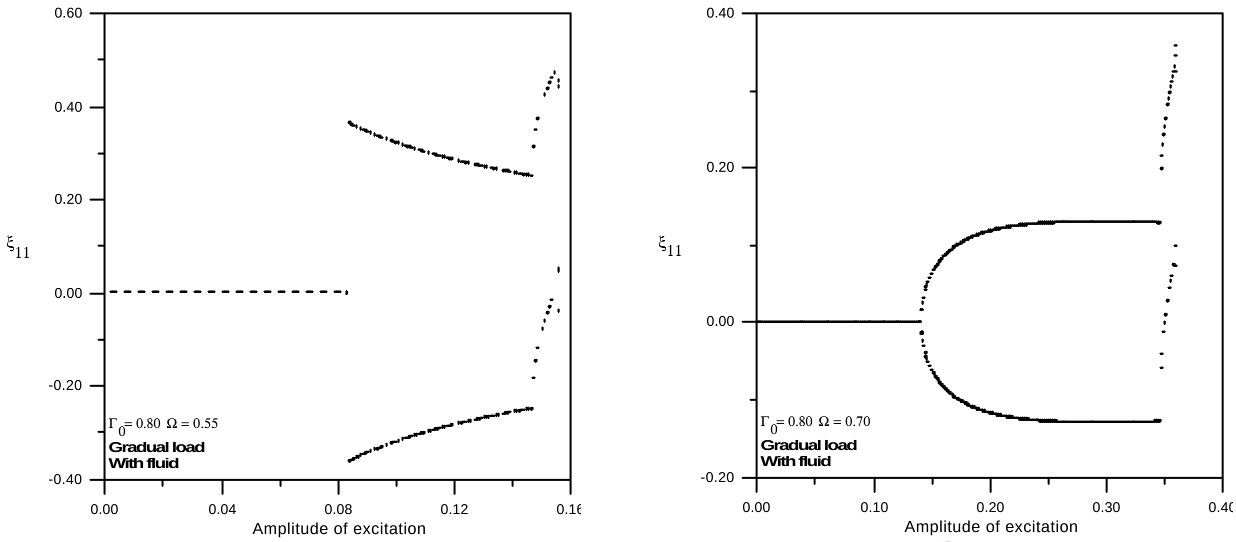

(c) (d)

Figure 4. Bifurcation diagrams of the Poincaré map for water filled shell. Principal instability region, Γ_o=0,80.

The bifurcation diagrams depicted in Figures 3.a and 4.a are typical of the left branch of the principal region of parametric instability. In this case, the bifurcation point corresponds to a sub-critical bifurcation of the trivial solution. For such sub-critical bifurcations the stability is suddenly lost and the system jumps to another stable solution. This leaves a regime where there is no attractor within the pre-buckling well after the critical point is reached and hence an inevitable jump to escape under increasing forcing occurs. This explains why in this region the numerically obtained parametric instability boundary practically coincides with the escape boundary.

In Figure 3.b, the jump is indeterminate. The response may re-stabilize within the well or jump to a remote attractor. The response that is attained physically depends on the initial conditions.

The bifurcation diagrams shown in Figures 3.c and 3.d are typical of the right, ascending branch of the stability boundary. When Γ_1 is lower than the critical value, the only possible steady state solution within the pre-buckling well is the trivial one, which is stable. Consequently, the response is trivial. When Γ_1 is greater than a critical value, there are two possible steady state solutions: (a) the trivial one, which is unstable; and (b) a finite amplitude period-two (2T) solution, which is stable. In this, case, since disturbances are always present, the response is non-trivial. Also, these figures show that as Γ_1 increases fom zero, the response consists of the trivial solution. As Γ_1 exceeds the critical value, ξ_{11} begins to increase slowly with increasing Γ_1. The critical value is in this case is a supercritical bifurcation point. As the amplitude of the forcing increases, the amplitude of the response increases until the escape boundary is reached. Before escape occurs, the period-two solution may also become unstable, being followed by a period doubling cascade, eventually reaching a narrow zone of chaotic motion, as illustrated in Figure 5.

Bifurcation diagrams in Figure 4 show a comportment similar to that described in Figure 3 but in this case for a pre-static load Γ_o=0,80.

If the cylinder is subjected to a periodic axial load, it will undergo the familiar longitudinal forced vibration, exhibiting a uniform transversal motion, due to the effect of Poisson's ratio, also know as breathing mode. However, at certain critical values, the longitudinal motion becomes unstable and the cylinder executes transverse bending vibrations. Figure 5 shows a representative time histories for Γo=0,80. Here $\Omega = \omega/\omega_o$ and ω_0 is the lowest natural frequency of the unloaded shell. A projection of the phase space and Poincaré section and is also shown in these figures. These figures were obtained by numerically integrating the equation of motion through the Runge-Kutta integration scheme. In Figure 5.a, for a forcing amplitude lower than a critical value Γ_1=0,12 and Ω = 0,70, after a finite initial disturbance, the amplitude of the response decreases rapidly converging to the trivial solution. In figure 5.b if the control parameter Γ_1 is increased beyond a critical value, the shell exhibits initially an exponential growth of the amplitude, converging to a limit cycle within the pre-buckling well. In this case, the trivial solution becomes unstable and the system converges to a period-two stable solution. In Figure 5.c when Γ_1 = 0,32 the shell exhibits initially a chaotic motion and finally jumps to a post-buckling configuration with a period two- stable solution. If, Γ_1 is increased still further, Γ_1 = 0,45, as shown in Figure 5.d, the shell exhibits a chaotic motion, oscillating about a post-buckling configuration.

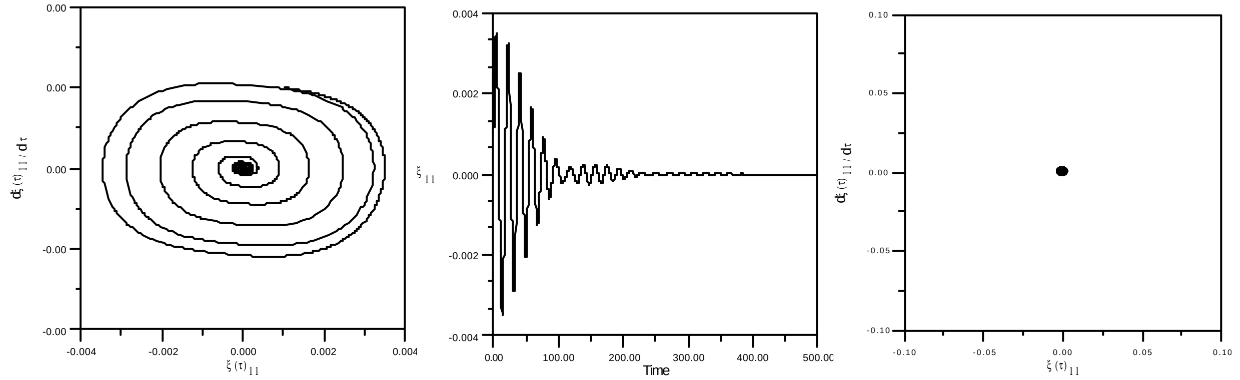

(a) Γ_1 = 0,12

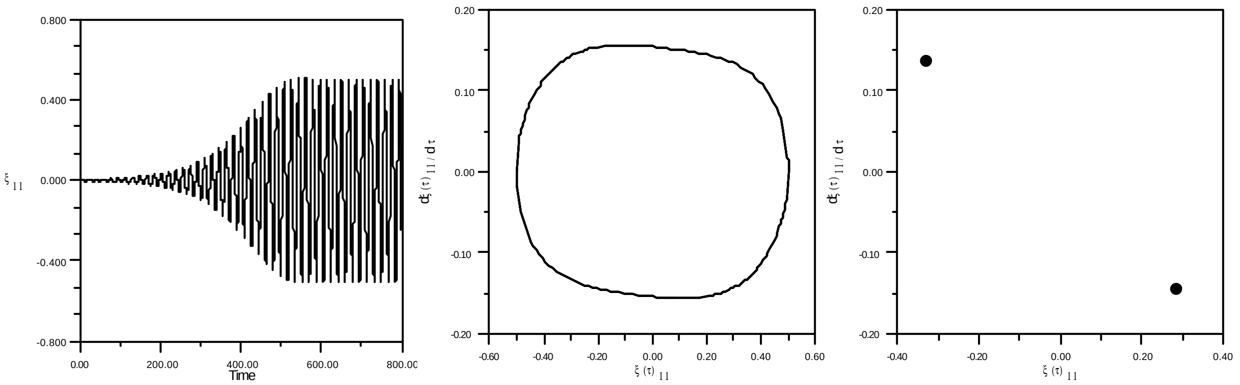

(b) Γ_1 = 0,16

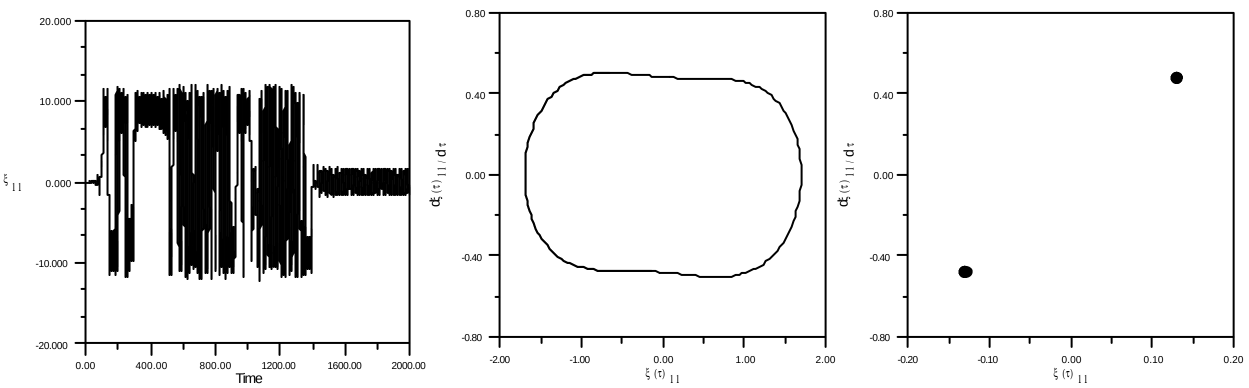

(c) Γ_1 = 0,30

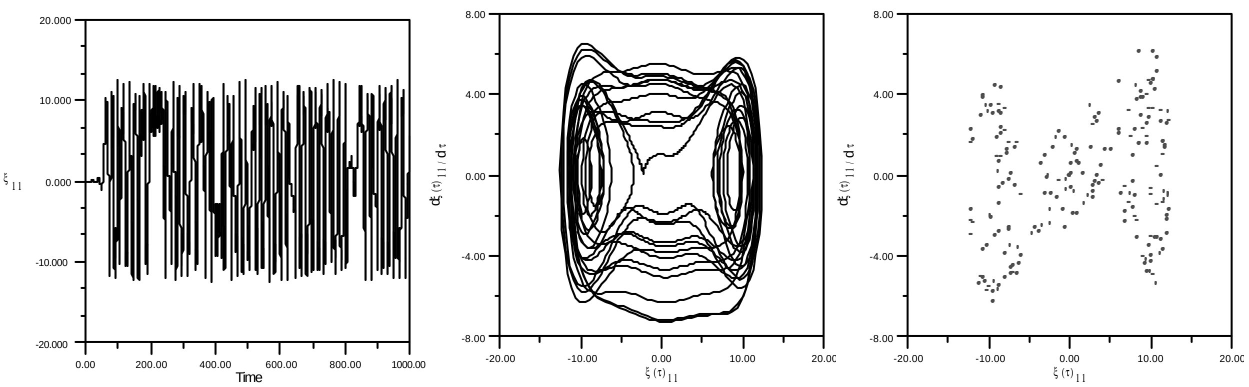

(d) Γ_1 = 0,45

Figure 5. Time response, phase plane and Poincaré section for Γ_o = 0,80 and Ω = 0,70.

4. Concluding remarks.

Based on Donnell's shallow shell equations, an accurate low-dimensional model is derived and applied to the study of the nonlinear vibrations of an axially loaded fluid filled circular cylindrical shell. The results show the influence of the modal coupling on the post-buckling response and on the nonlinear dynamic behavior of fluid filled circular cylindrical shells. Also the influence of a static compressive loading on the dynamic characteristics is investigated with emphasis on the parametric instability and escape from the pre-buckling potential well. The most dangerous region in parameter space is obtained and the triggering mechanisms associated with the stability boundaries are identified. The results show that the shell may exhibit several types of bifurcations. As a result, the engineer should exercise considerable care when designing fluid filled cylindrical shells under axial time- dependent loads.

5. References

Amabili, M., Pellicano, F. & Paï doussiss, M., 1998. "Nonlinear Vibrations of Simply Supported Circular Cylindrical Shells, Coupled to Quiescente Fluid". Journal of Fluids and Structures 12: 883-918.

Amabili, M., Pellicano, F. & Paï doussis, M. P., 2000. "Nonlinear vibrations of fluid-filled, simply supported circular cylindrical shells: theory and experiments". Nonlinear Dynamics Plates and Shells; AMD – Vol. 238: 73-84. New York: ASME.

Amabili, M., Pellicano, F. & Paï doussis, M. P., 2001. "Nonlinear supersonic flutter of circular cylindrical shells". AIAA J. 39: 564-573.

Boyarshina, L. G., 1984. "Resonace effects in the nonlinear vibrations of cylindrical shells containing a liquid". Soviet Applied Mechanics 20: 765-770.

Boyarshina, L. G., 1988. "Nonlinear wave modes of an elastic cylindrical shell partially filled with a liquid under conditions of resonance". Soviet Applied Mechanics 24: 528-534.

Chiba, M., 1993b. "Non-Linear Hydroelastic Vibration of a cantilever Cylindrical Tank". International Journal of Non-Linear Mechanics 28: 591-559.

Croll, J. G. A. & Batista, R. C., 1981. "Explicit Lower Bounds for the Buckling of Axially Loaded Cylinders". International Journal of Mechanical Science 23: 331-343.

Gonçalves, P. B. & Batista, R. C., 1988. "Non-Linear Vibration Analysis of Fluid-Filled Cylindrical Shells". Journal of Sound and Vibration 127: 133-143.

Gonçalves, P. B. & Del Prado, Z. J. G. N., 2000. "The role of modal coupling on the non-linear response of cylindrical shells subjected to dynamic axial loads". In: Nonlinear Dynamics of Plates and Shells; AMD – Vol. 238: 105-116. New York: ASME.

Gonçalves, P. B. & Del Prado, Z. J. G. N., 2002. "Nonlinear Oscillations ans Stability of Parametrically Excited Cylindrical Shells". Meccanica 37: 569-597.

Gonçalves, P. B. & Del Prado, Z. J. G. N., 2002. "Influence of Modal Interaction on the Parametric Instability of Cylindrical Shells". Structural Dynamics, EURODYN2002.

Hunt, G. W., Williams, K. A. J. & Cowell, R. G., 1986. "Hidden Symmetry Concepts in the Elastic Buckling of Axially Loaded Cylinders". International Journal of Solid and Structures 22: 1501-1515.

Ramachandran, J., 1979. "Nonlinear Vibrations of Cylindrical Shells of Varying Thickness in an Incompressible Fluid". Journal of Sound and Vibration 64: 97-106.

Yamaki, N., 1984. "Elastic Stability of Circular Cylindrical Shells". Amsterdam: North Holland.